

A direct measurement of the masses of ultra diffuse galaxies with weak gravitational lensing

Cristóbal Sifón^{1,2}, Remco F. J. van der Burg³, Henk Hoekstra² Adam Muzzin⁴ and Ricardo Herbonnet²

¹*Department of Astrophysical Sciences, Peyton Hall, Princeton University, Princeton, NJ 08544, USA*

²*Leiden Observatory, Leiden University, PO Box 9513, NL-2300 RA Leiden, Netherlands*

³*Laboratoire AIM, IRFU/Service d'Astrophysique - CEA/DSM - CNRS - Université Paris Diderot, Bât. 709, CEA-Saclay, 91191 Gif-sur-Yvette Cedex, France*

⁴*Department of Physics and Astronomy, York University, 4700 Keele St., Toronto, Ontario, Canada, M3J 1P3*

3 February 2017

ABSTRACT

The recent discovery of thousands of ultra diffuse galaxies (UDGs) in nearby galaxy clusters has opened a new window into the process of galaxy formation and evolution. Several scenarios have been proposed to explain the formation history of UDGs, and their ability to survive in the harsh cluster environments. A key requirement to distinguish between these scenarios is a measurement of their halo masses which, due to their very low surface brightnesses, has proven difficult if one relies on stellar tracers of the potential. We exploit weak gravitational lensing, a technique that does not depend on these baryonic tracers, to measure the average total mass of 909 UDGs selected in 21 clusters at $z \leq 0.09$. We constrain the average mass of subhaloes hosting UDGs to $\log m_{\text{UDG}}/M_{\odot} \leq 11.45$, within a radius $r \sim 40$ kpc, at 95 per cent confidence. Although uncertainties are large, this is inconsistent with them being failed L^* galaxies, and suggests that they are more likely to live in haloes that are more typical for regular dwarf galaxies.

1 INTRODUCTION

Large, low surface brightness galaxies have been known to exist both in the field (Dalcanton et al. 1997) and in galaxy clusters (Impey et al. 1988; Turner et al. 1993) for some time. A subset of these low surface brightness galaxies—dubbed ultra-diffuse galaxies (UDGs) by van Dokkum et al. (2015a)—has recently started receiving particular attention. UDGs stand out as the largest galaxies of their kind, with effective (or half-light) radii $r_{\text{eff}} \geq 1.5$ kpc, which are in fact typical of galaxies with masses similar to that of the Milky Way, $M \sim 10^{12} M_{\odot}$. In contrast, their stellar masses are only $M_{\star} \lesssim 10^8 M_{\odot}$, two orders of magnitude less than the Milky Way. A striking feature of UDGs is the fact that they are a numerous population in massive galaxy clusters (van Dokkum et al. 2015a; Koda et al. 2015; Mihos et al. 2015; Yagi et al. 2016; van der Burg et al. 2016).

Several hypotheses have been put forth to try to explain the unexpected survival of UDGs in massive clusters. In the initial discovery of UDGs in the Coma Cluster, van Dokkum et al. (2015a) suggested that UDGs may be failed L^* galaxies which fell into the cluster at early times, after having used only a small fraction of their cold gas to form stars. Once part of a cluster, their remaining cold gas was removed and they were left as very dark matter dominated galaxies. Yozin & Bekki (2015) have shown that such a mechanism can in fact produce UDG-like galaxies in hydrodynamical simulations. Alternatively, Amorisco & Loeb (2016) and Di Cintio et al. (2017) have suggested that the intrinsic properties of some dwarf galaxies are responsible for the formation of UDGs; if so, they should therefore be abundant in the field as well as in

clusters. However, a study of UDGs in the field is complicated by the lack of redshift information, whereas large numbers of UDGs that happen to be co-located in projection with galaxy clusters can safely be assumed to be part of the cluster (or at least a significant fraction of them; e.g., van der Burg et al. 2016). Furthermore, the one UDG with a spectroscopic redshift has been confirmed to be part of the Coma cluster (van Dokkum et al. 2015b).

Among the properties of UDGs that may shed light on the models above and others, their total mass is a crucial one. Knowing the masses of UDGs would allow us to unambiguously rule out some classes of hypotheses, such as the ‘failed L^* ’ hypothesis. In fact, there have been some attempts at estimating the masses of individual UDGs. Beasley et al. (2016) measured a velocity dispersion of globular clusters associated with a UDG in the Virgo Cluster of $33^{+16}_{-10} \text{ km s}^{-1}$ within 8.1 kpc, which suggests a virial mass¹ $m_{200} \sim 10^{11} M_{\odot}$. Similar masses have been estimated for a few UDGs indirectly from the number of globular clusters (Beasley & Trujillo 2016; Peng & Lim 2016). All these measurements suggest that UDGs are dwarf galaxies and not failed L^* galaxies. On the other hand, van Dokkum et al. (2016) estimated a virial mass $m \sim 10^{12} M_{\odot}$ from the stellar velocity dispersion and globular cluster count of a particularly large UDG ($r_{\text{eff}} = 4.5$ kpc). Such mass is

¹ Note that subhaloes cannot be physically assigned a virial mass, since they are embedded in the potential of the host cluster. However, referring to virial masses offers a convenient point for comparison. We therefore adhere to the use of virial masses in this discussion, but adopt a different mass definition in our analysis (see Section 3). See also the discussion in Sifón et al. (2017).

comparable to that of the Milky Way—possibly a failed L^* galaxy. Since all of the above mass estimations refer to single UDGs, it is not clear how they can be interpreted in the context of the UDG population, and therefore they are of limited use in distinguishing UDG formation hypothesis. Instead, measurements of the masses of a representative population of UDGs are required to draw conclusions about their origin.

Only weak gravitational lensing—the distortion of light from background galaxies by the mass distribution of objects closer to us—can provide direct measurements of *typical* masses of UDGs. Gravitational lensing does not rely on faint, low-surface brightness baryonic tracers of the mass in galaxies, and therefore provides a clear advantage over stellar dispersion measurements or globular cluster counts when trying to estimate UDG masses. For instance, the globular clusters identified by Beasley & Trujillo (2016) have magnitudes $m_{814} \gtrsim 26$ in the AB system, for a UDG in the *Coma Cluster*. Evidently, such an analysis would be extremely expensive for more distant objects.

The feasibility of weak lensing for measuring the total masses of satellite galaxies has already been demonstrated (e.g., Sifón et al. 2015a, 2017; Li et al. 2016). Here, we present the first direct constraints on the average masses of UDGs using measurements of weak lensing produced by UDGs in a sample of 21 clusters at $z \leq 0.09$ taken from the Multi-Epoch Nearby Cluster Survey (MENeCS, Sand et al. 2012). Throughout this work we adopt a flat Λ CDM model with $\Omega_m = 0.315$ and $H_0 = 70 \text{ km s}^{-1} \text{ Mpc}^{-1}$, consistent with the latest results of the *Planck* satellite (Planck Collaboration 2015).

2 DATA ANALYSIS

2.1 UDG sample

MENeCS is a multi-epoch survey of 57 clusters at $z \leq 0.15$ carried out with Megacam in the Canada-France-Hawaii Telescope (Sand et al. 2012). The data reduction is described in detail by van der Burg et al. (2013, 2016). The resulting full width at half maximum of the point spread function is less than 1 arcsec for all clusters in the sample, and the photometric zero points have been calibrated to about 0.01 mag. We consider 21 of those 57 clusters, located at $z \leq 0.09$, where we can still identify most UDGs given their surface brightness. These clusters have masses $M_{200} \gtrsim 10^{14} M_\odot$, as determined from galaxy velocity dispersions (Sifón et al. 2015b). We list our cluster sample in Table 1.

Following the original definition by van Dokkum et al. (2015a), van der Burg et al. (2016) identified UDGs in a subset of our clusters as galaxies with surface brightnesses within one effective radius of $24.0 \leq \langle \mu(r, r_{\text{eff}}) \rangle \leq 26.5$ and effective radii $1.5 \leq r_{\text{eff}}/\text{kpc} \leq 7.0$; these parameters were measured using GALFIT (Peng et al. 2002, 2010) to fit a single Sérsic profile to the light distribution. In order to have a sample that is as pure as possible but still obtain a large enough number of UDG candidates, van der Burg et al. (2016) considered eight clusters at $0.04 \leq z \leq 0.07$ and at galactic latitude $b \geq 25^\circ$. The study of van der Burg et al. (2016) is unique in that they did not select UDGs by visual inspection after the automatic selection based on structural parameters. While this has the disadvantage that the sample may be (and in fact is, as we show below) contaminated by artefacts of various kinds, it allows for an objective, statistically-consistent study of their properties after accounting for the expected number of such objects in control fields. This contamination however can significantly alter

Table 1. Cluster sample. Clusters masses, M_{200} , refer to the dynamical masses estimated by Sifón et al. (2015b), and r_{200} are the radii containing such masses. Note that here the overdensity is defined with respect to the critical density of the Universe. The last column lists the number of good UDG candidates after cleaning the sample by visual inspection, without correcting for further contamination, and the estimated number of interlopers in parentheses.

Cluster	Redshift	M_{200} ($10^{14} M_\odot$)	r_{200} (Mpc)	Number of UDGs
A85	0.055	10.2 ± 1.8	2.0 ± 0.1	97 (33)
A119	0.044	7.4 ± 1.2	1.8 ± 0.1	82 (17)
A133	0.056	5.5 ± 1.6	1.7 ± 0.2	78 (27)
A399	0.072	6.6 ± 2.0	1.8 ± 0.2	63 (12)
A401	0.074	8.9 ± 2.3	1.9 ± 0.2	57 (11)
A780	0.055	7.2 ± 2.7	1.8 ± 0.2	57 (25)
A1650	0.084	4.5 ± 0.9	1.5 ± 0.1	16 (9)
A1651	0.085	8.0 ± 1.3	1.9 ± 0.1	35 (13)
A1781	0.062	0.6 ± 0.3	0.8 ± 0.1	20 (9)
A1795	0.063	5.0 ± 0.9	1.6 ± 0.1	109 (30)
A1991	0.059	1.9 ± 0.5	1.2 ± 0.1	35 (14)
A2029	0.078	16.1 ± 2.5	2.4 ± 0.1	34 (19)
A2033	0.080	7.7 ± 2.0	1.8 ± 0.2	25 (13)
A2064	0.073	3.4 ± 1.7	1.4 ± 0.2	5 (5)
A2065	0.072	14.4 ± 2.5	2.3 ± 0.1	19 (13)
A2142	0.090	13.8 ± 1.2	2.2 ± 0.1	62 (20)
A2495	0.079	4.1 ± 0.8	1.5 ± 0.1	13 (6)
A2597	0.083	3.5 ± 2.0	1.4 ± 0.3	20 (8)
A2670	0.076	8.5 ± 1.2	1.9 ± 0.1	26 (11)
MKW3S	0.045	2.6 ± 0.5	1.3 ± 0.1	23 (8)
ZWCL1215	0.077	7.7 ± 1.7	1.9 ± 0.1	33 (11)

lensing measurements in a way that may not be fully captured by subtracting the signal from a control sample.

We therefore start from the sample compiled by van der Burg et al. (2016), but take some additional steps to define the sample used for weak lensing measurements. We first expand the cluster sample to $z \leq 0.09$ in order to increase the number of UDGs in our sample. We also impose stricter size cuts on the UDG sample $r_{\text{eff}} \geq 2.0 \text{ kpc}$ for $z \leq 0.07$ and $r_{\text{eff}} \geq 3.0 \text{ kpc}$ for higher redshifts, as we find that these cuts significantly reduce the contamination of the sample. Since most of the weak lensing signal is produced by the more massive UDGs in the first place, these two extra steps ensure a cleaner signal without losing information. Finally, we visually inspected all UDG candidates and only kept high-confidence UDG candidates. We classify a UDG candidate as high-confidence if it does not suffer significant blending with other galaxies; this ensures that the measured structural parameters are unbiased (i.e., without significant residuals in a model-subtracted image), but do not make any visual selection based on surface brightness, color or morphology. While this somewhat subjective selection could potentially bias statistical analyses such as that carried by van der Burg et al. (2016), it is essential for a clean interpretation of lensing measurements around the UDGs. Based on our visual inspection, we reject 14 per cent of the automatically-selected candidates. We show sample candidates and their ‘visual scores’ in the same format as they were inspected in ???. We also show the distributions of stellar mass and effective radii of our final sample of UDGs in Figure 1.

2.2 Weak lensing measurements

Our weak lensing analysis is identical in methodology to that presented in Sifón et al. (2017), which follows closely the cluster lens-

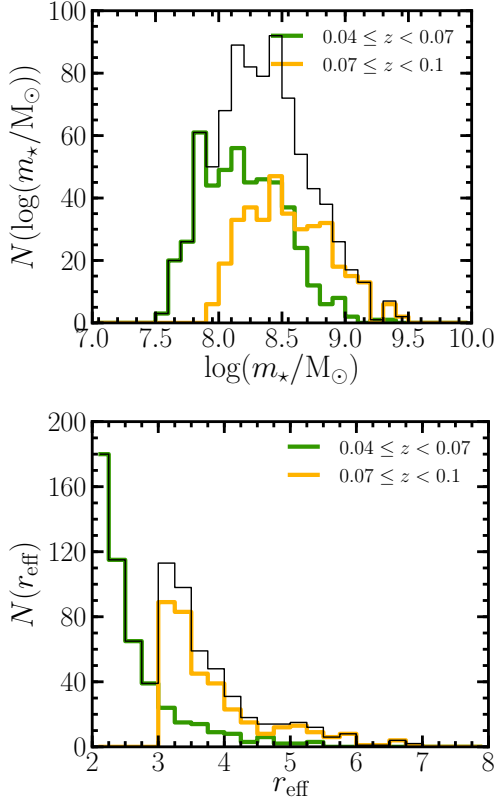


Figure 1. Distribution of stellar masses (top) and effective radii (bottom) of the UDG candidates that pass our visual inspection, split into a low (green) and high (orange) redshift samples. The thin black lines show the distribution for the full sample.

ing analyses of [Hoekstra et al. \(2015\)](#) and [Herbonnet et al. \(in prep.\)](#). The weak lensing signal is measured as an average tangential alignment, or shear, γ_t , of galaxies in the background of the lenses (in this case, UDGs) using the moments-based KSB algorithm ([Kaiser et al. 1995](#); [Luppino & Kaiser 1997](#); [Hoekstra et al. 1998](#)). The shear is closely related to the excess surface density, $\Delta\Sigma$,

$$\Delta\Sigma \equiv \bar{\Sigma}(< R) - \bar{\Sigma}(R) = \Sigma_c \gamma_t, \quad (1)$$

where $\bar{\Sigma}(< R)$ and $\bar{\Sigma}(R)$ are the average surface densities within a projected radius² R and within a thin shell around R , respectively, and Σ_c is a geometric factor accounting for the lensing efficiency,

$$\Sigma_c \equiv \frac{c^2}{4\pi G} \frac{D_s}{D_l D_{ls}}, \quad (2)$$

with D_s , D_l and D_{ls} being the angular diameter distances to the source, to the lens, and between the lens and the source. We calculate D_s and D_{ls} by matching the magnitude distribution of the source sample to photometric redshifts estimated from deep, multi-band observations, thus constructing a redshift distribution for the source sample (see [Herbonnet et al. in prep.](#)).

We define our source sample in an identical way to [Sifón et al. \(2017\)](#). We do not apply any colour cuts to the sample, but correct the lensing measurements with a ‘boost factor’ that accounts for

contamination by cluster members, which dilute the lensing signal. This boost factor has been calibrated using tailor-made image simulations in which each the red sequence galaxies of each cluster have been added to a simulation of the background source population, reproducing the noise and seeing properties of the real data ([Herbonnet et al. in prep.](#)). These simulations also allow us to assess obscuration of background galaxies by cluster galaxies, which biases the determination of the boost factor. In [Sifón et al. \(2017\)](#), we found a significant obscuration by typical satellite galaxies at scales $R \lesssim 20$ kpc. UDGs, however, have low surface brightness and do not produce any significant obscuration; instead we calculate the average obscuration as a function of cluster-centric distance, as in [Herbonnet et al. \(in prep.\)](#), to correct the boost factor. We also find that the tangential additive bias on the lensing measurements due to extended lens light, found to be about 30% at $R \sim 20$ kpc for typical satellites by ([Sifón et al. 2017](#)), is negligible for UDGs.

3 THE WEAK LENSING SIGNAL OF ULTRA DIFFUSE GALAXIES

3.1 Model for the UDG lensing signal

As described in detail in [Yang et al. \(2006\)](#) and [Sifón et al. \(2015a\)](#), the satellite lensing signal can be described by the sum of a subhalo and a host halo terms, both of which are essentially independent of each other. We model the average density profile of both UDGs and the host clusters as NFW profiles ([Navarro et al. 1995](#)). Following [Sifón et al. \(2017\)](#), we define the mass of subhaloes hosting UDGs, m_{bound} , as the bound subhalo mass—that is, the mass within the region where the density is above the background density of the cluster. In order to estimate the background density, we take the expected value for the three-dimensional radius based on the number density profile of normal cluster galaxies measured by [van der Burg et al. \(2015\)](#), which provides a good description of the distribution of UDGs outside $R_{\text{sat}} \sim 0.15r_{200}$. Specifically,

$$\langle r_{\text{UDG}} \rangle = \left[\int_{0.15c}^{\infty} d\chi \rho(\chi, c) \right]^{-1} \int_{0.15c}^{\infty} d\chi \chi \rho(\chi, c) = 0.38r_{200,h}, \quad (3)$$

where $\rho(x, c)$ is the NFW profile, with an adopted $c = 2$ for satellite galaxies (including UDGs) in MENeCS clusters ([van der Burg et al. 2015, 2016](#)). Our model therefore has four parameters: the average masses and concentrations of UDGs and the corresponding ones for host clusters. In practice, we are only able to constrain the masses of UDGs and their host clusters; we treat the concentrations as nuisance parameters.

We fit this model to the measurements using the affine-invariant Markov Chain Monte Carlo (MCMC) ensemble sampler *emcee* ([Foreman-Mackey et al. 2013](#)), fully accounting for the data covariance as described in [Sifón et al. \(2015a, 2017\)](#). We adopt flat priors for all parameters in the following ranges:

$$\begin{aligned} 8.5 &\leq \log(m_{200,\text{UDG}}/M_{\odot}) \leq 13.0 \\ 14.0 &\leq \log(M_{200,\text{cl}}/M_{\odot}) \leq 16.0 \\ 10 &\leq c_{\text{UDG}} \leq 20 \\ 2 &\leq c_{\text{cl}} \leq 8. \end{aligned} \quad (4)$$

The ranges chosen for the cluster and subhalo concentrations are informed by results from numerical simulations ([Dutton & Macciò 2014](#); [Moliné et al. 2016](#), respectively)

² As a convention, we list two-dimensional distances with upper case R and three-dimensional distances with lower case r .

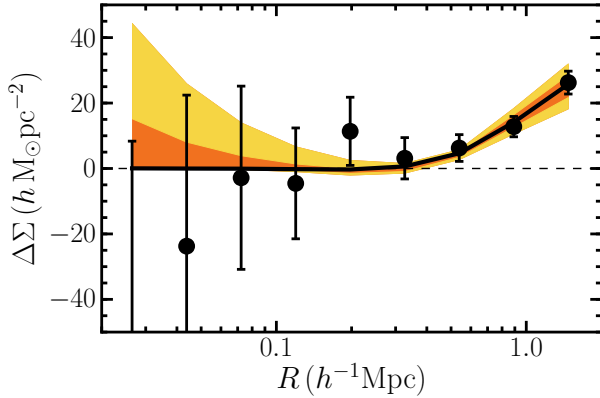


Figure 2. Lensing signal of ultra-diffuse galaxies in clusters at $z \leq 0.09$. Orange and yellow regions show the 68 and 95 per cent credible intervals from the MCMC sampling, while the black line shows the best-fit model.

3.2 Constraints on the average UDG mass

We show in **Figure 2** the lensing signal of our sample of UDGs, along with the best-fit model. Our model constrains the ‘virial’ mass of subhaloes to $\log m_{200}/M_\odot \leq 11.94$ at 95 per cent credibility. At an average cluster-centric distance of $\langle r_{\text{UDG}} \rangle = 0.38 r_{200,\text{cl}}$, this results in a bound mass $\log m_{\text{bound}}/M_\odot \leq 11.45$ within a radius $r_{\text{bound}} = 41^{+41}_{-37}$ kpc at 95 per cent credibility. The wide range in r_{bound} is given by the range in allowed host cluster masses, which changes both the background density and the value of $r_{200,\text{cl}}$. The best-fit host cluster mass is $\log M_{\text{cl}}/M_\odot = 14.96^{+0.11}_{-0.11}$ (68 per cent credible interval).

These results are somewhat dependent on the range chosen for c_{UDG} , with lower concentrations allowing for higher subhalo masses. However, it is unlikely that subhaloes would have concentrations much lower than $c = 10$ —these are in fact the typical concentrations of host haloes of these masses (e.g., [Dutton & Macciò 2014](#); [Moliné et al. 2016](#)).

To allow a comparison with recent measurements of UDG masses from stellar dynamics and globular clusters, we also report the upper limit for the mass within 10 kpc, $m_{<10\text{kpc}} \leq XX M_\odot$, but we note that this value is an extrapolation of the data—a result of the adopted NFW profile.

4 DISCUSSION

Weak gravitational lensing measures the total mass irrespective of its nature. The median stellar mass of UDGs in our sample is $\langle m_\star \rangle = 2.0 \times 10^8 M_\odot$. Thus their dark matter fraction can be as high as 99.9 per cent, although we are not able to detect mass in excess of the stellar mass. Lensing has the advantage compared to stellar dynamics that it probes the total masses of galaxies, instead of the masses within the small radii within which velocity dispersions can be measured (e.g., roughly 8 kpc in the case of DF17 in the Coma cluster [Beasley & Trujillo 2016](#); [Peng & Lim 2016](#)), and therefore allows a more straightforward comparison with other kinds of galaxies, without the need for an extrapolation of the density profile from ~ 8 kpc to tens of kpc (although lensing also relies to some extent on an assumed density profile).

However, weak lensing has therefore the disadvantage that the total and stellar masses are measured at very different radii, and the question of how dark matter-dominated these galaxies are, compared to dwarf or ‘normal’ galaxies, is difficult to address.

Our weak lensing measurements suggest the typical UDG (with $\langle r_{\text{eff}} \rangle \sim 3$ kpc) resides in a dark matter halo that contains at most half the mass of the Milky Way. This supports the idea that UDGs are dwarfs, as opposed to failed L^\star galaxies. This is in agreement with the mass suggested by globular cluster counts in a $r_{\text{eff}} = 2.5$ kpc UDG in the Coma cluster ([Beasley & Trujillo 2016](#); [Peng & Lim 2016](#)). On the other hand, [van Dokkum et al. \(2016\)](#) estimated a virial mass of about $10^{12} M_\odot$ for DF44 (also in Coma). This UDG has a stellar mass $m_\star \sim 3 \times 10^8 M_\odot$, similar to the average stellar mass in our sample, but an effective radius $r_{\text{eff}} \sim 4.5$ kpc, not representative of UDGs in general. The total mass inferred by [van Dokkum et al. \(2016\)](#) suggests either that DF44 is an outlier, compared to the population of UDGs, in terms of its total-to-stellar mass ratio, or that the assumed extrapolation from a dynamical mass of $7 \times 10^9 M_\odot$ within 4.6 kpc to a virial mass of $\sim 10^{12} M_\odot$ is not valid. For this extrapolation, [van Dokkum et al. \(2016\)](#) assumed a concentration of $c \sim 10$ ([Macciò et al. 2008](#)), at the low end of our chosen range. As discussed above, lowering the concentration tends to increase the mass allowed by our lensing measurements, and this may partly explain the fact that we consider DF44 an outlier. A study of the velocity dispersion of a statistical sample of UDGs may help understand this difference.

Our upper limit on the mass of UDGs suggests that they are not strong outliers in the total-to-stellar mass relation of cluster galaxies, as measured by [Sifón et al. \(2017\)](#). So far, theoretical scenarios in which UDGs are dwarf galaxies also require an abundant field UDG population. A study of field UDGs would face the additional challenge that it would be very difficult to determine their redshifts in large numbers.

make plot like right panel of fig 8 with the UDG upper limit

REFERENCES

- Amorisco N. C., Loeb A., 2016, *MNRAS*, **459**, L51
 Beasley M. A., Trujillo I., 2016, preprint, ([arXiv:1604.08024](#))
 Beasley M. A., Romanowsky A. J., Pota V., Navarro I. M., Martinez Delgado J., Neyer F., Deich A. L., 2016, *ApJL*, **819**, L20
 Dalcanton J. J., Spergel D. N., Gunn J. E., Schmidt M., Schneider D. P., 1997, *AJ*, **114**, 635
 Di Cintio A., Brook C. B., Dutton A. A., Macciò A. V., Obreja A., Dekel A., 2017, *MNRAS*, **466**, L1
 Dutton A. A., Macciò A. V., 2014, *MNRAS*, **441**, 3359
 Foreman-Mackey D., Hogg D. W., Lang D., Goodman J., 2013, *PASP*, **125**, 306
 Hoekstra H., Franx M., Kuijken K., Squires G., 1998, *ApJ*, **504**, 636
 Hoekstra H., Herbonnet R., Muzzin A., Babul A., Mahdavi A., Viola M., Cacciato M., 2015, *MNRAS*, **449**, 685
 Impey C., Bothun G., Malin D., 1988, *ApJ*, **330**, 634
 Kaiser N., Squires G., Broadhurst T., 1995, *ApJ*, **449**, 460
 Koda J., Yagi M., Yamanoi H., Komiyama Y., 2015, *ApJL*, **807**, L2
 Li R., et al., 2016, *MNRAS*, **458**, 2573
 Luppino G. A., Kaiser N., 1997, *ApJ*, **475**, 20
 Macciò A. V., Dutton A. A., van den Bosch F. C., 2008, *MNRAS*, **391**, 1940
 Mihos J. C., et al., 2015, *ApJL*, **809**, L21
 Moliné Á., Sánchez-Conde M. A., Palomares-Ruiz S., Prada F., 2016, preprint, ([arXiv:1603.04057](#))
 Navarro J. F., Frenk C. S., White S. D. M., 1995, *MNRAS*, **275**, 720
 Peng E. W., Lim S., 2016, *ApJL*, **822**, L31
 Peng C. Y., Ho L. C., Impey C. D., Rix H.-W., 2002, *AJ*, **124**, 266
 Peng C. Y., Ho L. C., Impey C. D., Rix H.-W., 2010, *AJ*, **139**, 2097
 Planck Collaboration 2015, preprint, ([arXiv:1502.01589](#))
 Sand D. J., et al., 2012, *ApJ*, **746**, 163
 Sifón C., et al., 2015a, *MNRAS*, **454**, 3938

- Sifón C., Hoekstra H., Cacciato M., Viola M., Köhlinger F., van der Burg R. F. J., Sand D. J., Graham M. L., 2015b, *A&A*, **575**, A48
- Sifón C., Herbonnet R., Hoekstra H., Cacciato M., van der Burg R. F. J., Viola M., Sand D. J., Graham M. L., 2017, in preparation
- Turner J. A., Phillipps S., Davies J. I., Disney M. J., 1993, *MNRAS*, **261**, 39
- Yagi M., Koda J., Komiyama Y., Yamanoi H., 2016, *ApJS*, **225**, 11
- Yang X., Mo H. J., van den Bosch F. C., Jing Y. P., Weinmann S. M., Meneghetti M., 2006, *MNRAS*, **373**, 1159
- Yozin C., Bekki K., 2015, *MNRAS*, **452**, 937
- van Dokkum P. G., Abraham R., Merritt A., Zhang J., Geha M., Conroy C., 2015a, *ApJL*, **798**, L45
- van Dokkum P. G., et al., 2015b, *ApJL*, **804**, L26
- van Dokkum P., et al., 2016, preprint, ([arXiv:1606.06291](https://arxiv.org/abs/1606.06291))
- van der Burg R. F. J., et al., 2013, *A&A*, **557**, A15
- van der Burg R. F. J., Hoekstra H., Muzzin A., Sifón C., Balogh M. L., McGee S. L., 2015, *A&A*, **577**, A19
- van der Burg R. F. J., Muzzin A., Hoekstra H., 2016, *A&A*, **590**, A20